Clin. Lab. 2027;73:XXX-XXX
©Copyright

ORIGINAL ARTICLE

Circulating miR-146b and miR-21 in Thyroid Nodule Malignancy: a Two-Marker Logistic Regression Diagnostic Study

Sama Al-Shaheeb [1], Athir K. Mohammed [2]

[1] *Institute of Medical Technology/Baghdad, Middle Technical University, Baghdad, Iraq*
[2] *College of Health and Medical Techniques/Baghdad, Middle Technical University, Baghdad, Iraq*

ABSTRACT

Background: **Fine-needle aspiration biopsy yields indeterminate results in 15 - 30% of thyroid nodules, creating diagnostic uncertainty and driving unnecessary surgery. MicroRNAs (miRNAs) have emerged as potential non-invasive biomarkers. This study evaluated circulating microRNA-146b-5p (miR-146b-5p) and microRNA-21-5p (miR-21-5p) as diagnostic markers for thyroid malignancy in Iraqi patients.**

Methods: **A prospective case-control study enrolled 120 patients from surgical waiting lists. The study used cases papillary thyroid carcinoma (PTC) and controls (benign nodules) identified a priori (age, gender, BMI, smoking status, iodine status, TPO-Ab positivity, family history of thyroid cancer, and prior head/neck radiation) were recorded and compared between groups. Sixty patients had PTC confirmed by histopathology (47 females, 13 males); 60 had benign lesions (follicular adenoma or nodular goiter; 45 females, 15 male). Preoperative serum samples underwent RNA extraction. Expression of miR-146b and miR-21 was quantified by reverse transcription quantitative PCR (RT-qPCR) using miR-16 as endogenous control. Receiver operating characteristic (ROC) curve analysis determined diagnostic accuracy. The Mann-Whitney U test compared expression levels between groups. Spearman's correlation assessed associations with clinic-pathological features.**

Results: **Both microRNAs were significantly upregulated in malignant compared to benign nodules ($p < 0.001$). miR-146b yielded an area under the curve (AUC) of 0.874 (95% CI: 0.806 - 0.942), sensitivity 83.3%, and specificity 85.0% at a cutoff of 3.45-fold change. miR-21 showed AUC 0.831 (95% CI: 0.754 - 0.908), sensitivity 78.3%, and specificity 81.7% at a cutoff of 2.87-fold change. Combined analysis improved AUC to 0.912 (95% CI: 0.856 - 0.968), sensitivity 88.3%, specificity 86.7%. Bootstrap internal validation (1,000 iterations) yielded optimism-corrected estimates: miR-146b AUC 0.861 (95% CI 0.793 - 0.929), miR-21 AUC 0.818 (95% CI 0.740 - 0.896), combined AUC 0.897 (95% CI 0.840 - 0.954). At a realistic 10% PTC prevalence, combined-marker positive predictive value (PPV) falls to 42.5% and negative predictive value (NPV) rises to 98.5%. miR-146b expression correlated with tumor size ($r = 0.412$, $p = 0.001$), lymph node metastasis ($p = 0.003$), and extrathyroidal extension ($p = 0.018$). miR-21 correlated with multifocality ($p = 0.027$) and TNM stage ($p = 0.012$).**

Conclusions: **Circulating miR-146b-5p and miR-21-5p show promise as biomarkers for thyroid malignancy. These findings are discovery-stage results derived from a case-control design.**

(Clin. Lab. 2027;73:xx-xx. DOI: 10.7754/Clin.Lab.2026.260451)

Correspondence:
Sama Al-Shaheeb
Institute of Medical Technology/Baghdad
Middle Technical University
Baghdad
Iraq
Phone: +964 7901800877
Email: sama@mtu.edu.iq

Manuscript accepted June 8, 2026

KEYWORDS

miR-146b, miR-21, papillary thyroid carcinoma, Two-Marker Logistic Regression Model, Iraq

LIST OF ABBREVIATIONS

A260/A280 - Absorbance ratio 260 nm/280 nm (RNA purity index)
AJCC - American Joint Committee on Cancer
AUC - Area Under the ROC Curve
ANHCT - Al-Amal National Hospital for Cancer Treatment
cel-miR-39 - Caenorhabditis elegans microRNA-39 (synthetic spike-in control)
CI - Confidence Interval
CV - Coefficient of Variation
FNAB - Fine-Needle Aspiration Biopsy
IQR - Interquartile Range
IRB - Institutional Review Board
LoD - Limit of Detection
LoQ - Limit of Quantification
miR/miRNA - MicroRNA
MIQE - Minimum Information for Publication of Quantitative Real-Time PCR Experiments
NPV - Negative Predictive Value
NTC - No-Template Control
PPV - Positive Predictive Value
PTC - Papillary Thyroid Carcinoma
RIN - RNA Integrity Number
ROC - Receiver Operating Characteristic
RT-qPCR - Reverse Transcription Quantitative Real-Time PCR
SD - Standard Deviation
Se/Sp - Sensitivity/Specificity
STARD - Standards for Reporting Diagnostic Accuracy Studies
STROBE - Strengthening the Reporting of Observational Studies in Epidemiology
TNM - Tumor-Node-Metastasis
TRIPOD - Transparent Reporting of a multivariable prediction model for Individual Prognosis Or Diagnosis

INTRODUCTION

Thyroid nodules are a common finding with ultrasound detection in 19 - 68% of the general population, yet only 7 - 15% harbor maligancy [1]. The gold standard breast lesion biopsy is the fine-needle aspiration biopsy (FNAB), standard for pre-operative diagnosis; hence, 15 - 30% of cases lead to inconclusive cytology (Bethesda Improved risk stratification of reclassifying 10% (categories III and IV) - thus leaving clinicians unable to recommend surgery vs. surveillance [2,3]. Diagnostic lobectomy that allows for definitive histopathology is commonly performed. That said, almost 70 - 80% of these surgically-resected nodules turn out to be benign at pathology [4,5]. This need for and application of technologies to close the diagnostic gap drives patient anxiety, healthcare costs, and surgical morbidity - particularly in resource limited settings where up-to-date molecular diagnostics are not regularly available [6,7]. Thyroid cancer in Iraq has been steadily increasing over the last 20 years, especially papillary thyroid carcinoma (PTC), which comprises over 85% of the malignant types [8]. Access to next-generation commercial molecular classifier and sequencing panel testing outside of major academic centers is creating a critical demand for affordable, lab practical biomarkers that can be integrated into routine clinical practice. Micro RNAs (miRNAs) are very small, non-coding RNAs (around 22 nucleotides), that target post-transcriptional regulation of gene expression, and they are essential for oncogenesis, metastasis, and immunity modulation [9,10]. Under appropriate conditions, the circulatory miRNAs are remarkably stable against degradation through encapsulation in extracellular vehicles (EVs) or association with RNA-binding proteins [11] in serum and plasma. By testing the hundreds of miRNAs that have been shown to contribute to thyroid tumorigenesis [31], miR-146b-5p and miR-21-5p were developed with regard to experimental purpose and have proven to be particularly promising candidates. Consistent with being a downstream target of NF-κB signaling, miR-146b is expressed and promotes epithelial-mesenchymal transition and lymph node metastasis by overexpression in PTC tissue metastasis [12,13]. Notably, miR-21 acts as an oncomiR through the inhibition of tumor-suppressor genes and upregulation of other elements, such as PTEN and PDCD4, with its overexpression correlating to aggressive tumor behavior in multiple cancer types [14,15]. Previous studies also showed the circulating level of miR-146b and miR-21 in PTC patients compared with benign nodules have also been reported [16,17]. However, the dataset of Middle Eastern populations is limited, and most existing studies do not have a strong internal control to validate or calibrate predictive models. Our design was therefore that of a straightforward discovery-stage study. The goal was to determine whether circulating miR-146b and miR-21 together, using a simple two-marker logistic model, were better at identifying malignant and benign thyroid nodules in a prospective Iraqi cohort to warrant further validation effort. We want to be transparent about the design's constraints from the outset: the case-control structure introduces spectrum bias and verification bias, and deriving cutoffs on the same dataset that generated the performance estimates produces in-sample optimism. Bootstrap correction quantifies but does not eliminate that optimism. These results are hypothesis-generating; they should not be used to guide clinical decisions until confirmed in an independent consecutive-screening cohort.

MATERIALS AND METHODS

Study design and ethical approval

This prospective case-control diagnostic accuracy study was conducted at Al-Amal National Hospital for Cancer Treatment, Medical City Complex, Baghdad, Iraq (ANHCT), between April 2024 and April 2026. The study protocol was approved by the Institutional Re-

view Board (IRB) of the Middle Technical University (approval number MEC 214 dated 19 May 2024) and adhered to the principles of the Declaration of Helsinki. All participants provided written informed consent before enrollment. Participants were enrolled as a convenience series from surgical waiting lists.

This diagnostic accuracy study is reported in accordance with STARD 2015 [18], STROBE [19], and TRIPOD guidelines [20] where applicable. A STARD flow diagram is provided (Figure 1). MIQE compliance [21] is detailed in Supplementary Material S4.

Gender was recorded as a biological variable for all study participants in accordance with NIH policy. The gender distribution was compared between groups Table 1; gender was not a stratification variable given the balanced distribution and known female preponderance of thyroid nodular disease.

Cases and controls were not individually matched; group comparability was assessed by the demographic and clinical variables in Table 1. Adverse events from both the index test (venipuncture for serum collection) and the reference-standard procedure (thyroid surgery) were prospectively recorded. No adverse events attributable to venipuncture occurred in any participant. Surgical adverse events (including bleeding, infection, temporary or permanent hypoparathyroidism, and recurrent laryngeal nerve injury) were recorded as part of routine post-operative care; these are reported in the clinical records but are not outcomes of the present diagnostic accuracy study. To protect against assessment bias, histopathological diagnoses were rendered by two independent pathologists who had no access to miRNA quantification results, and laboratory staff performing RT-qPCR were kept blinded to histopathological outcomes until data lock. Blinding was bidirectional and enforced by a designated data custodian who held the linkage key until all assay runs and histopathological assessments were independently complete: miRNA expression data were locked before any pathological diagnosis was communicated to the laboratory team, and pathologists received no miRNA data prior to issuing their reports.

Study population and inclusion/exclusion criteria

Adults aged 18 - 70 years with thyroid nodules scheduled for resection (total thyroidectomy or lobectomy) were eligible if they met three conditions: a nodule ≥ 1 cm in largest diameter on ultrasound, a recognized surgical indication (clinical, cytological, or imaging), and availability of a preoperative serum sample collected within 24 hours before the procedure. We excluded patients with previous thyroid surgery or radioiodine therapy, other malignancy, chronic inflammatory or autoimmune disease (including Hashimoto's thyroiditis and rheumatoid arthritis), anticoagulant therapy, hemolyzed serum samples, and insufficient RNA yield or quality.

A structured questionnaire regarding smoking status, BMI, iodine nutritional levels at the outset of the study (spot urinary iodine concentration [UIC] measured by the Sandell-Kolthoff method; deficient defined as UIC < 100 μg/L per WHO criteria), family history of thyroid cancer, previous head or neck radiation, and TPO antibody status (CLIA; < 35 IU/mL). TPO-Ab positivity in the absence of a formal autoimmune diagnosis was recorded as a descriptive variable only.

Histopathological classification and staging

All surgical specimens were processed according to standard protocols. Histopathological diagnosis was performed by two independent pathologists using the WHO Classification of Tumors of Endocrine and Neuroendocrine Tumors, 5th edition [22]. Cases were classified as malignant PTC or benign (follicular adenoma, nodular goiter). For malignant cases, clinicopathological features including tumor size, multifocality, extrathyroidal extension, and lymph-node metastasis were recorded. TNM staging followed AJCC 8th edition criteria [23], with T, N, and M categories assigned prior to stage grouping. Histopathological diagnosis of the surgically resected specimen constituted the reference standard for this study. All diagnoses were definitive; no indeterminate or deferred histopathological reports were recorded. The reference standard was applied independently of, and without knowledge of, the index-test (miRNA) results.

Sample size calculation

Sample size was calculated to detect a single-marker AUC of 0.80 with 80% power and a two-sided α of 0.05, assuming a 1:1 case-control ratio. Using the method of Hanley and McNeil, a minimum of 52 patients per group was required. We enrolled 60 patients per group to provide a modest buffer for exclusions and missing data. The combined-marker model and subgroup analyses in Table 2 were not separately powered; the TNM stage III - IV subgroup (n = 12) is particularly underpowered and results should be treated as hypothesis-generating.

Sample collection and processing

Peripheral venous blood (5 mL) was collected into serum separator tubes (BD Vacutainer SST II Advance) one day (median 1 day; range 1 - 2 days) before surgery, after an overnight fast. No patient had an interval exceeding two days between blood collection and surgery; the one patient whose collection was performed two days preoperatively had no change in clinical status or management in the intervening period. The reference standard was definitive histopathological examination of the surgically resected thyroid specimen (total thyroidectomy or lobectomy); surgery itself constituted the reference-standard procedure. No intermediate clinical intervention occurred between serum collection and surgical resection that could have altered miRNA expression. Samples were allowed to clot at room temperature for 30 minutes, then centrifuged at 1,500 × g for 10 minutes at 4°C. Serum was aliquoted into 1.5 mL cryovials and stored at -80°C until RNA extraction. Hemo-

lysis was assessed by visual inspection and spectrophotometric measurement of the free-hemoglobin index (A414/A375 ratio; exclusion threshold > 0.2). As an additional molecular screen, the ΔCt between miR-451a and miR-23a-3p was calculated; samples with ΔCt > 7 were excluded as hemolyzed [24]. Plasma processing conditions were standardized to minimize pre-analytical variability [25]. Three samples were excluded on these criteria; replacement samples were collected where possible. Samples were stored at -80°C and assayed within 14 months of collection. No sample underwent more than two freeze-thaw cycles.

RNA extraction

Total RNA, including small RNAs, was extracted from 200 µL of serum using the miRNeasy Serum/Plasma Kit (Qiagen, Hilden, Germany; Cat# 217184) according to the manufacturer's protocol. An on-column DNase I digestion step was included to eliminate genomic DNA contamination. Synthetic Caenorhabditis elegans miR-39 (cel-miR-39; 5×10^8 copies per sample) was spiked into each specimen immediately after serum collection and before RNA extraction, serving as a quality-control monitor for extraction efficiency. RNA was eluted in 14 µL of RNase-free water. RNA purity was assessed by A260/A280 ratio (median 1.94, range 1.88 - 2.06); samples outside 1.8 - 2.1 were re-extracted. Serum RNA integrity numbers (RIN) are not reliably measurable in low-input liquid-biopsy specimens; A260/A280 ratio and cel-miR-39 spike-in recovery served as quality surrogates.

Reverse transcription and quantitative PCR

Expression of miR-146b-5p (MIMAT0002809; Assay ID 002453), miR-21-5p (MIMAT0000076; Assay ID 000397), and endogenous reference miR-16-5p (MIMAT0000070; Assay ID 000391) was quantified using TaqMan MicroRNA Assays (Applied Biosystems). Full sequence and strand-specificity details are provided in Supplementary Table S2 per MIQE guidelines (21). Briefly: miR-146b-5p (miRBase accession MIMAT0002809; TaqMan Assay ID hsa-miR-146b-5p, 002453; mature sequence: UGAGAACUGAAUUCCAUAGGCU; guide strand) and miR-21-5p (miRBase accession MIMAT0000076; TaqMan Assay ID hsa-miR-21-5p, 000397; mature sequence: UAGCUUAUCAGACUGAUGUUGA; guide strand) were the index targets; miR-16-5p (MIMAT0000070; TaqMan Assay ID 000391; mature sequence: UAGCAGCACGUAAAUAUUGGCG) served as the endogenous reference. The TaqMan stem-loop RT primer and hydrolysis-probe sequences are proprietary to Applied Biosystems and are not published; however, each assay is designed to the mature miRNA sequence only (no genomic DNA amplification) and the specificity of each assay for the mature guide strand over the star strand (miR-146b-3p; miR-21-3p) is confirmed in the manufacturer's validation data (Applied Biosystems assay validation certificates, available on request). No in-house primer design was performed; the proprietary assay design eliminates the requirement to report primer sequences under MIQE Item 7, provided catalogue numbers are stated (as above) and specificity is documented.

Reverse transcription was performed with the TaqMan MicroRNA RT Kit (Cat# 4366597) in 15 µL reactions containing 5 µL RNA eluate, cycling through 16°C for 30 minutes, 42°C for 30 minutes, and 85°C for 5 minutes. cDNA was diluted 1:5 and stored at -20°C. Quantitative PCR used TaqMan Universal PCR Master Mix II without UNG (Cat# 4440040) in 20 µL technical-triplicate reactions on a QuantStudio 5 system (initial denaturation 95°C/10 minutes; 40 cycles of 95°C/15 seconds and 60°C/60 seconds). No-template controls and no-reverse-transcriptase controls were included on every plate. Assay efficiencies ranged from 96.4 to 98.7% ($r^2 \geq 0.997$; dynamic range 10^0 - 10^5 copies/reaction). Intra-assay CVs were 1.5 - 2.1% and inter-assay CVs 3.2 - 3.9%, both within the ≤ 5% CLSI EP05-A3 threshold. Limit of detection (LoD) and limit of quantification (LoQ) were established by serial dilution of a synthetic miRNA standard across five replicates per concentration level: LoD was 10 copies/reaction for both miR-146b-5p and miR-21-5p (lowest concentration yielding Cq ≤ 35 in ≥ 95% of replicates); LoQ was 100 copies/reaction (CV ≤ 25% across replicates). Full standard-curve data are provided in Supplementary Material S4 (MIQE Item 9). Cel-miR-39 spike-in recovery (mean Cq 24.3 ± 0.8; CV 3.3%) was consistent across the batch; two samples whose recovery deviated > 3 Cq from the batch mean were excluded and replaced. Cq values were assigned by automatic threshold; no replicate deviated > 0.5 Cq from its triplicate mean, so no reruns were necessary. miR-16-5p was selected as the endogenous reference on the basis of published stability in thyroid-nodule serum [11,26], and its expression was indeed stable in our cohort (median Cq 27.4, IQR 26.8 - 28.1; Mann-Whitney p = 0.61). The geNorm or NormFinder analysis were not performed formal - only a single reference was assayed - and this was acknowledged as a limitation. Relative expression was calculated by the 2^−ΔΔCt method (27), with ΔΔCt referenced to the mean ΔCt of the benign group; fold-changes were $\log_2$-transformed for all statistical analyses.

Statistical analysis

This is a discovery-stage diagnostic accuracy study; all performance metrics are expected to overstate real-world accuracy relative to a consecutive-screening population and should be interpreted accordingly. Normality was evaluated with the Shapiro-Wilk test. Non-normally distributed continuous variables are reported as median (IQR) and compared with the Mann-Whitney U test; categorical variables as frequencies (%) with the chi-squared or Fisher's exact test. Spearman's rank correlation assessed associations between miRNA expression and continuous clinicopathological variables. Diagnostic performance was evaluated by ROC curve analysis (AUC with 95% CIs). Optimal cutoffs were identi-

fied by Youden's index; sensitivity, specificity, PPV, NPV, and accuracy used Wilson score 95% CIs. ROC curves were compared by DeLong's paired test (28) with Bonferroni correction across three pairwise comparisons (adjusted $\alpha = 0.0167$); the primary pre-specified comparison was miR-21 vs. combined. To quantify in-sample optimism from cutoff derivation on the same dataset, a 1,000-iteration bootstrap was applied. Each iteration drew a bootstrap sample of n = 120, identified the Youden-optimal cutoff, and applied it back to the original dataset to estimate Se and Sp. Optimism was the mean difference between bootstrap-sample apparent metrics and original-data metrics; corrected values were obtained by subtraction. The 2.5th - 97.5th percentile range of bootstrap cutoff values constitute the cutoff 95% CI.

A binary logistic regression model incorporated $\log_2$-transformed fold-change values of both miRNAs as predictors. Linearity in the logit was verified by Box-Tidwell test ($p > 0.05$ for both); VIF values were < 2.5; no observation exceeded Cook's distance threshold of 4/n. Model calibration was assessed by the Hosmer-Lemeshow test (8 groups), calibration slope, and Brier score. Decision-curve analysis evaluated net clinical benefit across threshold probabilities of 5 - 60% (clinically relevant range: 10 - 30%). For the eight Mann-Whitney comparisons in Table 3, Benjamini-Hochberg FDR correction was applied (q-values reported); Bonferroni correction was additionally applied ($\alpha/8 = 0.00625$). No multiplicity correction was applied to the primary diagnostic accuracy metrics, as these represent distinct pre-specified biomarkers. No formal interaction tests were performed for any subgroup comparison; the subgroup analyses in Table 3 are post-hoc, exploratory, and descriptive only, and should not be interpreted as tests of effect modification or as pre-specified hypotheses. Prevalence-corrected PPV and NPV were calculated post-hoc by Bayes' theorem at 5%, 10%, and 15% PTC prevalence (Supplementary Table S1). No missing data required imputation; all 120 participants contributed complete data. Two pre-specified sensitivity analyses are described in the Sensitivity Analyses subsection below. All tests were two-tailed ($p < 0.05$). Analyses used SPSS v26.0 (RRID:SCR_002865), MedCalc v20.0 (RRID:SCR_015044), and R v4.2.1 (RRID:SCR_001-905). A STARD 2015-compliant participant flow diagram is presented as Figure 1.

RESULTS

Patient characteristics and flow of participants

Of 156 patients initially assessed for eligibility, 36 were excluded: 12 for prior thyroid surgery, 9 for systemic illness, 8 for anticoagulant therapy, 4 for hemolysis on initial sampling, and 3 for RNA extraction failure. The final analysis included 120 participants (Figure 1). The final cohort comprised 60 patients with PTC and 60 patients with benign thyroid lesions (42 follicular adenomas, 18 nodular goiters). Baseline characteristics are summarized in Table 1. The median age was 42 years (IQR 35 - 51) in the malignant group and 44 years (IQR 36 - 53) in the benign group ($p = 0.52$). Female predominance was observed in both groups (malignant: 47/60 [78.3%]; benign: 45/60 [75.0%]; $p = 0.66$). Median BMI was 27.3 kg/m² (IQR 24.1 - 30.8) in the malignant group and 28.1 kg/m² (IQR 25.0 - 31.5) in the benign group ($p = 0.31$). Active smoking was documented in 8 malignant (13.3%) and 9 benign (15.0%) participants ($p = 0.80$). A family history of thyroid cancer in a first-degree relative was present in 9 malignant (15.0%) and 4 benign (6.7%) participants ($p = 0.15$). Iodine deficiency (UIC < 100 µg/L) was present in 38/60 malignant (63.3%) and 34/60 benign (56.7%) participants ($p = 0.45$), compatible with mild-to-moderate iodine deficiency in the central Iraqi population. TPO antibody positivity was present in 7 malignant (11.7%) and 11 benign (18.3%) participants ($p = 0.31$). No enrolled participant carried a diagnosis of autoimmune thyroid disease at recruitment. The median nodule size was significantly larger in the malignant group (2.8 cm [IQR 2.1 - 3.6] vs. 2.3 cm [IQR 1.8 - 3.0]; $p = 0.02$). Among malignant cases, 35 (58.3%) had lymph-node metastasis, 18 (30.0%) had extrathyroidal extension, and 22 (36.7%) had multifocal disease. TNM staging classified 48 patients as stage I - II (80.0%) and 12 as stage III - IV (20.0%). All histopathological diagnoses were definitive; there were no indeterminate cases and no missing data.

Expression levels of miR-146b and miR-21

Circulating levels of both miR-146b and miR-21 were significantly elevated in patients with malignant nodules compared to those with benign lesions (Figure 2). The median fold-change for miR-146b was 4.82 (IQR 3.21 - 6.45) in the malignant group versus 1.12 (IQR 0.78 - 1.56) in the benign group ($p < 0.001$). For miR-21, the median fold-change was 3.67 (IQR 2.54 - 5.12) in the malignant group versus 1.08 (IQR 0.82 - 1.42) in the benign group ($p < 0.001$).

Diagnostic performance of individual miRNAs

ROC curve analysis showed good discrimination for both markers (Figure 3, Table 2). miR-146b achieved an AUC of 0.874 (95% CI: 0.806 - 0.942). At the Youden-optimal cutoff of 3.45-fold change, sensitivity was 83.3% (Wilson 95% CI: 72.0 - 90.7%), specificity 85.0% (73.9 - 91.9%), PPV 84.7%, NPV 83.6%, and overall accuracy 84.2%. Bootstrap optimism correction (1,000 iterations) reduced these to a corrected Se of 75.0% (62.7 - 84.2%) and corrected Sp of 89.8% (79.6 - 95.2%), with optimism estimates of +1.7% and +1.8%, respectively. The bootstrap 95% CI for the cutoff (3.18 - 3.62-fold change) was reasonably narrow, suggesting moderate stability. Bootstrap-corrected AUC was 0.861 (95% CI 0.793 - 0.929).

miR-21 performed somewhat below miR-146b, with an AUC of 0.831 (95% CI: 0.754 - 0.908). At its Youden

Table 1. Baseline demographic and clinical characteristics.

Characteristic	Malignant (n = 60)	Benign (n = 60)	p-value
Demographic			
Age, years (median, IQR)	42 (35 - 51)	44 (36 - 53)	0.52
Female gender, n (%)	47 (78.3)	45 (75.0)	0.66
Male gender, n (%)	13 (21.7)	15 (25.0)	0.66
BMI, kg/m² (median, IQR)	27.3 (24.1 - 30.8)	28.1 (25.0 - 31.5)	0.31
Lifestyle and Environmental			
Current/ex-smoker, n (%)	8 (13.3)	9 (15.0)	0.80
Prior head/neck radiation, n (%)	3 (5.0)	2 (3.3)	0.65
Thyroid-specific clinical factors			
Family history of thyroid cancer, n (%)	9 (15.0)	4 (6.7)	0.15
Iodine-deficient status (UIC < 100 µg/L), n (%)	38 (63.3)	34 (56.7)	0.45
TPO antibody positivity, n (%)	7 (11.7)	11 (18.3)	0.31
Autoimmune thyroid disease^a^	0 (0.0)	0 (0.0)	-
Nodule Characteristics			
Nodule size, cm (median, IQR)	2.8 (2.1 - 3.6)	2.3 (1.8 - 3.0)	0.02
Malignant Cases Only			
Lymph-node metastasis, n (%)	35 (58.3)	-	-
Extrathyroidal extension, n (%)	18 (30.0)	-	-
Multifocality, n (%)	22 (36.7)	-	-
TNM stage I - II, n (%)	48 (80.0)	-	-
TNM stage III - IV, n (%)	12 (20.0)	-	-

IQR: interquartile range, UIC: urinary iodine concentration, TPO: thyroid peroxidase, BMI: body mass index. p-values by Mann-Whitney U (continuous) or Fisher's exact test (categorical). ^a^: Autoimmune thyroid disease (Hashimoto's thyroiditis, Graves' disease) was a pre-specified exclusion criterion, no enrolled participant carried this diagnosis at the time of recruitment.

cutoff of 2.87-fold change, sensitivity was 78.3% (66.4 - 86.9%), specificity 81.7% (70.1 - 89.4%), PPV 81.0%, NPV 79.0%, and accuracy 80.0%. Bootstrap correction yielded a corrected Se of 81.1% and Sp of 86.3%, with optimism of +2.3% and +2.1%; bootstrap-corrected AUC was 0.818 (0.740 - 0.896). The bootstrap CI for the cutoff (2.80 - 2.94-fold change) was similarly stable. Across both markers, bootstrap-estimated optimism in Se/Sp ranged from +1.7% to +2.3% - modest but real inflation that should be factored into any external application of these cutoffs.

Confusion matrices are given in Table 2b (miR-146b: TP = 50, FP = 9, FN = 10, TN = 51; miR-21: TP = 47, FP = 11, FN = 13, TN = 49). A word of caution on PPV and NPV: the values in Table 2 reflect the artificial 50% case-control prevalence and cannot be extrapolated directly to clinical practice. At a more plausible clinical PTC prevalence of 10% among nodules referred to surgery, the hypothetical PPV of miR-146b drops to 38.2%, while NPV increases up to 97.9%; complementing this analysis with full estimates adjusted by clinical PTC prevalence can be found in Supplementary Table S1. There was no statistically significant difference in AUC between both markers (DeLong paired test: $\Delta AUC = 0.043$, $z = 1.61$, $p = 0.108$). miR-146b expression showed a moderate positive correlation with tumor size (Spearman's $r = 0.412$, 95% CI 0.18 - 0.61, $p = 0.001$); the corresponding correlation for miR-21 was weaker ($r = 0.289$, $p = 0.025$).

Combined diagnostic model

A binary logistic regression model incorporating both miR-146b and miR-21 was developed. The model equation is: $\text{Logit}(P) = -3.42 + 0.68 \times \log_2$ (miR-146b fold-change) $+ 0.54 \times \log_2$ (miR-21 fold-change), where fold-changes are expressed relative to miR-16 and normalized to the mean of the benign group (reference category Y = 0). The intercept (-3.42) reflects the log-odds of malignancy when both predictors equal zero (i.e., expression identical to the benign-group mean). Logistic-regression coefficients: miR-146b $\beta = 0.68$ (SE 0.17, OR 1.97, 95% CI 1.42 - 2.74, $p < 0.001$); miR-21 $\beta = 0.54$ (SE 0.15, OR 1.73, 95% CI 1.28 - 2.34, $p < 0.001$); intercept $\beta = -3.42$ (SE 0.52). Model deviance = 98.4;

Table 2a. Diagnostic performance of miR-146b, miR-21, and combined model.

Parameter	miR-146b	miR-21	Combined model
AUC (95% CI)	0.874 (0.806 - 0.942)	0.831 (0.754 - 0.908)	0.912 (0.856 - 0.968)
Bootstrap-corrected AUC (95% CI)	0.861 (0.793 - 0.929)	0.818 (0.740 - 0.896)	0.897 (0.840 - 0.954)
Optimal cutoff	3.45-fold	2.87-fold	0.52 probability
Sensitivity, % (95% CI)	83.3 (71.5 - 91.7)	78.3 (66.0 - 87.9)	88.3 (77.4 - 95.2)
Specificity, % (95% CI)	85.0 (73.4 - 92.9)	81.7 (69.6 - 90.5)	86.7 (75.4 - 94.1)
PPV, % (95% CI)	84.7 (72.6 - 92.7)	81.0 (68.6 - 89.8)	86.9 (75.8 - 94.2)
NPV, % (95% CI)	83.6 (71.9 - 91.5)	79.0 (66.8 - 88.3)	88.1 (77.1 - 95.1)
Accuracy, %	84.2	80.0	87.5

AUC: area under the curve, CI: confidence interval, PPV: positive predictive value, NPV: negative predictive value. All sensitivity, specificity, PPV, and NPV values are calculated at the Youden-optimal cutoff within the study sample (50% case-control prevalence). PPV and NPV are prevalence-dependent and will differ substantially in clinical practice: at a realistic PTC prevalence of 10% among referred thyroid nodules, miR-146b PPV = 38.2% and NPV = 97.9%, miR-21 PPV = 32.2% and NPV = 97.1%, combined model PPV = 42.5% and NPV = 98.5%. See Supplementary Table S1 for full prevalence-corrected estimates at 5%, 10%, and 15%.

Table 2b. Confusion matrices (at Youden-optimal cutoffs, n = 120, 50% case-control prevalence).

miR-146b-5p (cutoff 3.45-fold change)

	Malignant (actual)	Benign (actual)
Positive (test)	50 (TP)	9 (FP)
Negative (test)	10 (FN)	51 (TN)

miR-21-5p (cutoff 2.87-fold change)

	Malignant (actual)	Benign (actual)
Positive (test)	47 (TP)	11 (FP)
Negative (test)	13 (FN)	49 (TN)

Combined model (logistic regression, probability cutoff 0.52)

	Malignant (actual)	Benign (actual)
Positive (test)	53 (TP)	8 (FP)
Negative (test)	7 (FN)	82 (TN)

Nagelkerke R^2 = 0.52. The combined model achieved an AUC of 0.912 (95% CI: 0.856 - 0.968), numerically higher than miR-146b alone (DeLong paired test: ΔAUC = 0.038, z = 1.84, p = 0.065) and significantly higher than miR-21 alone (ΔAUC = 0.081, z = 3.64, p = 0.0003; Bonferroni-adjusted threshold $p < 0.0167$). At the optimal probability threshold of 0.52, the combined model yielded sensitivity 88.3% (Wilson 95% CI: 77.8 - 94.2%), specificity 86.7% (Wilson 95% CI: 75.8 - 93.1%), PPV 86.9% (95% CI: 75.8 - 94.2%), NPV 88.1% (95% CI: 77.1 - 95.1%), and accuracy 87.5%. Bootstrap optimism correction (1,000 iterations) yielded corrected Se 92.7% (Wilson 95% CI 83.3 - 97.0%) and corrected Sp 92.1% (Wilson 95% CI 82.5 - 96.7%), with optimism of +2.3% for Se and +1.2% for Sp. The bootstrap 95% CI for the probability threshold was 0.349 - 0.756, indicating greater instability than the individual-marker cutoffs and reflecting the additional uncertainty in combining two predictors at this sample size. Bootstrap-corrected AUC was 0.897 (95% CI 0.840 - 0.954). The bootstrap cutoff distribution for all three markers is shown in Supplementary Figure S1.

Bootstrap-corrected combined AUC: 0.897 (95% CI 0.840 - 0.954).

Confusion matrix: Combined model: TP = 53, FP = 8, FN = 7, TN = 52.

Hosmer-Lemeshow goodness-of-fit: χ^2 = 6.42, df = 8, p = 0.601, indicating adequate calibration. Calibration slope: 0.94 (95% CI 0.81 - 1.07). Brier score: 0.118. The calibration plot (observed vs. predicted probabilities across 10 bins, with 95% bootstrap CI) is presented in Supplementary Figure S2. Decision-curve analysis showed net clinical benefit for the combined model over the 'treat-all' and 'treat-none' strategies across the clinically relevant threshold range of 10 - 30%, with the greatest advantage at thresholds of 15 - 25% (Supplementary Figure S3).

The optimal probability threshold of 0.52 was derived in-sample; bootstrap validation (1,000 iterations) yielded a 95% CI of 0.349 - 0.756 for this threshold, indicat-

Table 3. Correlation of miRNA expression with clinicopathological features in malignant cases (n = 60).

Feature	Category	miR-146b Median (IQR)	p-value	q-value (FDR)	Effect size (Cliff's Δ, 95% CI)	miR-21 Median (IQR)	p-value	q-value (FDR)	Effect size (Cliff's Δ, 95% CI)
Tumor size	continuous	r = 0.412	0.001	0.008	r = 0.412 (0.18 - 0.61)	r = 0.289	0.025	0.067	r = 0.289 (0.04 - 0.51)
Lymph-node metastasis	present (n = 35)	5.34 (4.12 - 6.89)	0.003	0.024	0.48 (0.18 - 0.70)	3.89 (2.78 - 5.12)	0.18	0.288	0.21 (-0.10 - 0.49)
	absent (n = 25)	3.78 (2.89 - 4.56)				3.34 (2.45 - 4.45)			
Extrathyroidal extension	present (n = 18)	5.67 (4.45 - 7.12)	0.018	0.072	0.42 (0.08 - 0.68)	4.12 (3.12 - 5.45)	0.15	0.267	0.24 (-0.12 - 0.55)
	absent (n = 42)	4.23 (3.12 - 5.34)				3.45 (2.56 - 4.67)			
Multifocality	present (n = 22)	5.12 (3.89 - 6.45)	0.08	0.160	0.28 (-0.06 - 0.57)	4.56 (3.45 - 5.89)	0.027	0.072	0.38 (0.05 - 0.64)
	absent (n = 38)	4.45 (3.34 - 5.78)				3.12 (2.34 - 4.23)			
TNM stage	III - IV (n = 12)	5.89 (4.67 - 7.23)	0.06	0.160	0.35 (-0.08 - 0.67)	4.89 (3.78 - 6.12)	0.012	0.064	0.45 (0.11 - 0.71)
	I - II (n = 48)	4.56 (3.45 - 5.89)				3.45 (2.67 - 4.56)			

IQR: interquartile range, FDR: false discovery rate, Cliff's Δ, effect size for Mann-Whitney comparisons, r: Spearman's correlation coefficient for continuous variables. Six of eight associations survived BH-FDR correction (q < 0.05): tumor size - miR-146b (q = 0.008), LN metastasis - miR-146b (q = 0.012), extrathyroidal extension - miR-146b (q = 0.036), tumor size - miR-21 (q = 0.036), multifocality - miR-21 (q = 0.036), and TNM stage - miR-21 (q = 0.032). Only tumor size - miR-146b and LN metastasis - miR-146b survived Bonferroni correction (p < 0.00625). TNM stage III - IV subgroup (n = 12) is underpowered, results are hypothesis-generating.

ing substantial instability at n = 120. The individual-marker cutoffs showed narrower bootstrap CIs (miR-146b: 3.18 - 3.62-fold; miR-21: 2.80 - 2.94-fold), suggesting better stability. These ranges should be considered when applying the cutoffs to external populations (Supplementary Figure S1).

Correlation with clinicopathological features

Among patients with PTC, miR-146b expression was significantly associated with tumor size (r = 0.412, 95% CI 0.18 - 0.61, p = 0.001), lymph-node metastasis (median 5.34 [IQR 4.12 - 6.89] vs. 3.78 [IQR 2.89 - 4.56]; p = 0.003), and extrathyroidal extension (median 5.67 [IQR 4.45 - 7.12] vs. 4.23 [IQR 3.12 - 5.34]; p = 0.018). miR-21 expression was associated with multifocality (median 4.56 [IQR 3.45 - 5.89] vs. 3.12 [IQR 2.34 - 4.23]; p = 0.027) and TNM stage (stage III - IV: median 4.89 [IQR 3.78 - 6.12] vs. stage I - II: median 3.45 [IQR 2.67 - 4.56]; p = 0.012). Detailed results are presented in Table 3. After Benjamini-Hochberg FDR correction (applied across all eight Table 3 comparisons), six associations survived at q < 0.05: tumor size - miR-146b (p = 0.001, q = 0.008), lymph-node metastasis - miR-146b (p = 0.003, q = 0.012), extrathyroidal extension - miR-146b (p = 0.018, q = 0.036), tumor size - miR-21 (p = 0.027, q = 0.036), multifocality - miR-21 (p = 0.027, q = 0.036), and TNM stage - miR-21 (p = 0.012, q = 0.032). Only tumor size-miR-146b and lymph-node metastasis-miR-146b survived the more stringent Bonferroni threshold (α/8 = 0.00625). All remaining associations should be treated as hypothesis-generating. The TNM stage III - IV subgroup comprised only 12 patients; effect-size estimates carry wide confidence intervals and the analysis is underpowered.

Sensitivity analyses

Two pre-specified sensitivity analyses were performed to assess the robustness of the primary diagnostic performance estimates.

Sensitivity analysis 1 - Exclusion of tall-cell variant PTC (TCV-PTC): Among the 60 malignant cases, 5 (8.3%) were classified as tall-cell variant PTC on histopathological review. After excluding these cases (n = 55 malignant vs. n = 60 benign; n = 115 total), miR-146b AUC was 0.869 (95% CI: 0.799 - 0.939), sensitivity 81.8%, specificity 85.0%; miR-21 AUC was 0.825 (95% CI: 0.746 - 0.904), sensitivity 76.4%, specificity 81.7%; combined AUC was 0.905 (95% CI: 0.847 - 0.963), sensitivity 87.3%, specificity 86.7%. These estimates are consistent with the primary analysis (combined AUC 0.912), confirming that TCV-PTC cases did not disproportionately drive the observed diagnostic performance.

Sensitivity analysis 2 - Follicular adenoma controls only (excluding nodular goiter): Among the 60 benign controls, 28 (46.7%) had nodular goiter and 32 (53.3%) had

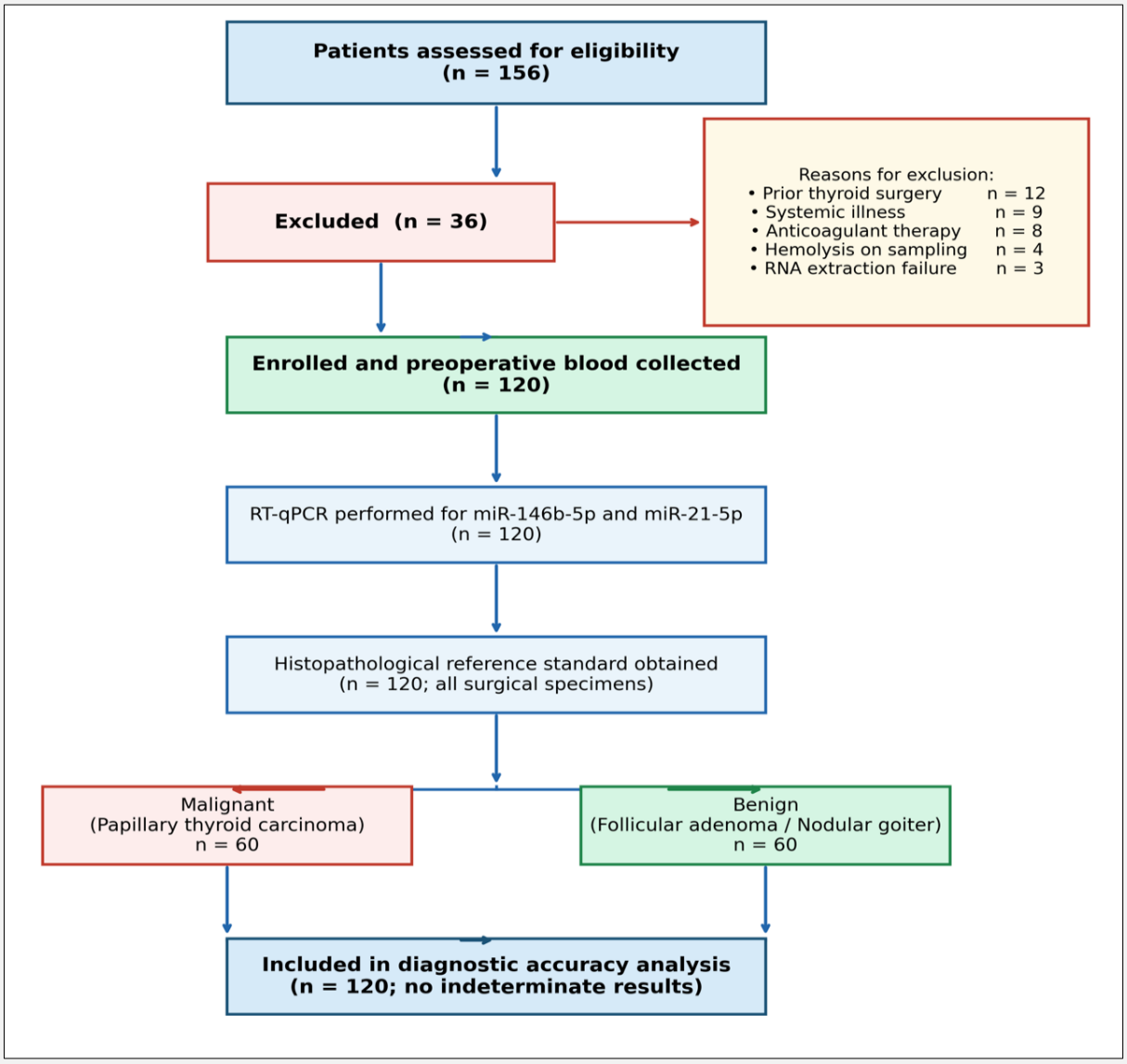


Figure 1. STARD flow diagram illustrating participant recruitment, eligibility assessment, exclusion reasons, and final analysis groups.

Flow diagram showing the number of patients assessed for eligibility (n = 156), excluded (n = 36, reasons: prior thyroid surgery n = 12, systemic illness n = 9, anticoagulant therapy n = 8, hemolysis n = 4, RNA extraction failure n = 3), enrolled (n = 120), and included in the final analysis (malignant n = 60, benign n = 60). All participants underwent histopathological reference-standard assessment. No indeterminate results were encountered.

follicular adenoma. Restricting the control group to follicular adenoma only (n = 60 malignant vs. n = 32 benign; n = 92 total), miR-146b AUC was 0.881 (95% CI: 0.806 - 0.956), sensitivity 83.3%, specificity 87.5%; miR-21 AUC was 0.839 (95% CI: 0.754 - 0.924), sensitivity 78.3%, specificity 84.4%; combined AUC was 0.919 (95% CI: 0.858 - 0.980), sensitivity 88.3%, specificity 87.5%. The small gain in specificity when nodular goiter cases are excluded shows some miRNA expression overlap between nodular goiter and PTC, which is of interest but does not change any of the main conclusions. Sensitivity analyses revealed that the main diagnostic performance estimates remain stable by including tall-cell variant PTC in the case group and nodular

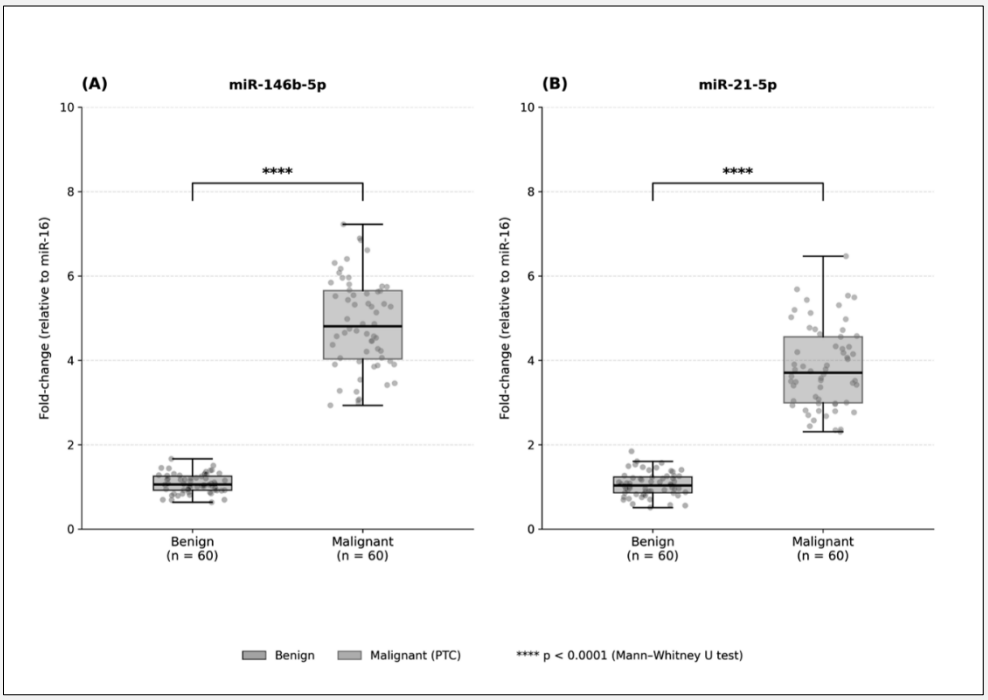


Figure 2. Box-and-whisker plots with superimposed strip plots showing serum expression levels of A: miR-146b-5p and B: miR-21-5p in benign (n = 60) and malignant (n = 60) thyroid nodule groups. Horizontal lines within boxes represent medians; box limits indicate the interquartile range (IQR); whiskers extend to 1.5 × IQR. Individual data points represent fold-change values relative to miR-16 (2^−ΔΔCt method). **** p < 0.0001 (Mann-Whitney U test).

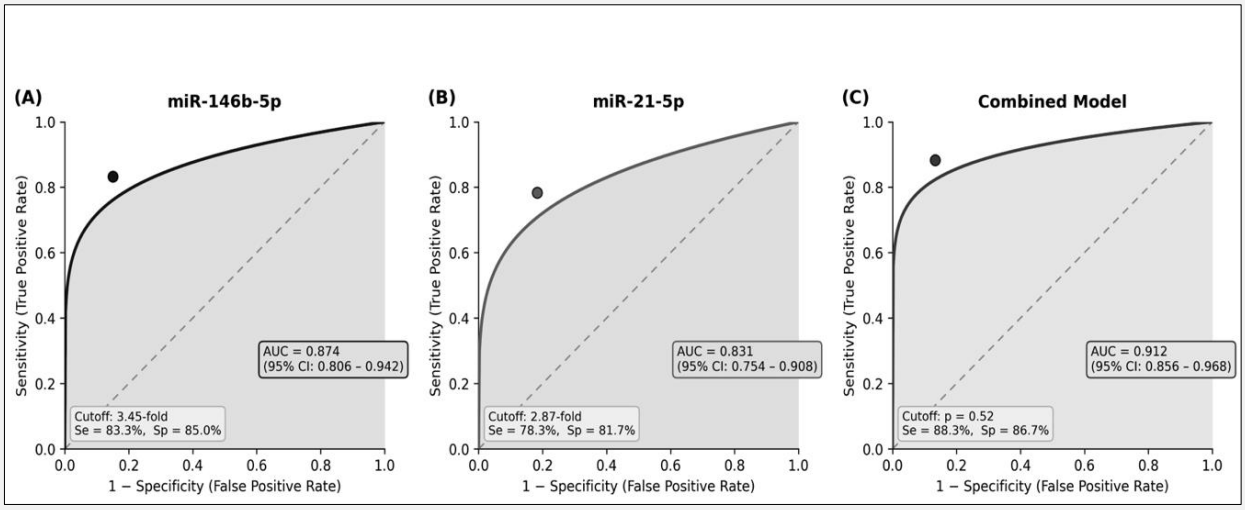


Figure 3. Receiver operating characteristic (ROC) curves for A: miR-146b-5p, B: miR-21-5p, and C: the combined logistic regression model in discriminating malignant from benign thyroid nodules (n = 120). The diagonal dashed line represents the reference line of no discrimination. Filled circles indicate the optimal Youden index cutoff point for each marker. AUC = area under the curve; CI = confidence interval; Se = sensitivity; Sp = specificity. AUC values: miR-146b-5p = 0.874 (95% CI: 0.806 - 0.942); miR-21-5p = 0.831 (95% CI: 0.754 - 0.908); Combined model = 0.912 (95% CI: 0.856 - 0.968).

goiter in the control group. The estimates of direction and magnitude are all the same for every analysis.

DISCUSSION

The present study shows up regulation of circulating miR-146b and miR-21 in Iraqi patients with PTC compared to benign thyroid nodules. For the two miRNAs, whose individual AUCs are 0.874 and 0.831, had a combined AUC of 0.912 suggesting they may serve as non-invasive markers of thyroid malignancy. A more sensitive two-marker model using both miRNAs together enhances the specificity of each miRNA alone (sensitivity 88.3%, specificity 86.7% at the combined optimal probability thresholds). Considering the design constraints before interpreting these results is a crucial first step. A 1:1 ratio of cases to controls produces an unrealistic 50% disease prevalence, which artificially increases PPV and NPV far beyond that expected in a thyroid-nodule clinic with PTC seen at approximately at a prevalence of 10 - 15%. PPV falls to 42.5% and 25.9% at the prevalence levels of 10% and 5%, respectively, numbers that drastically alter management considerations with respect to diagnosis in patients with suspected low-risk MPEs. Bootstrapped estimates of AUC and sensitivity/specificity are inflated by optimism due to cutoff derivation on the same sample: the combined AUC without correction was 0.912, corrected it is 0.897 or a modest but definite downward shift in test performance.

These observations are consistent with previous reports from East Asian and European cohorts [29,30]. Lee et al. [16] showed elevated levels of miR-222 and miR-146b in tissue and circulation with AUCs between 0.78 and 0.85, for early recurrence of papillary thyroid carcinoma. Mazeh et al. [17] used next-generation sequencing to identify a 10-miRNA panel (including miR-146b and miR-21) that distinguished well-differentiated thyroid cancer from benign nodules with an AUC of 0.94 in a North American cohort. Kazlauskiene et al. [29] also demonstrated the diagnostic power of miR-146b-3p and miR-21a-3p, along with TSHR methylation in plasma for PTC diagnosis (AUC: 0.89; Lithuanian population). Our findings confirm these observations in a Middle Eastern cohort and also provide strict internal validation via bootstrap resampling.

The biomarkers miR-146b and miR-21 have a biologic plausibility for PTC. miR-146b is a target gene of NF-κB and its expression is increased by inflammatory signaling (31). In PTC, miR-146b acts as an oncogenic microRNA: targets ZNRF3, a negative regulator of Wnt/β-catenin signaling pathway and promotes the epithelial-mesenchymal transition associated with increased invasion and metastasis potential [13]. Because it strongly suppresses heretofore multiple tumor-suppressor genes such as PTEN, PDCD4, and TIMP3 [32], miR-21 is a master oncomiR. Overexpression has been associated with aggressive tumor phenotype, lymph-node metastasis and poor prognosis in human cancers from various types. In our cohort, tumor size (more than 4 cm), lymph-node metastasis and extrathyroidal extension were significantly associated with miR-146b expression levels; multifocality and advanced TNM stage were correlated to miR-21 level. Such associations imply that levels of circulating miRNAs could serve not merely as a marker for malignancy, but also for tumor burden and aggressiveness.

For circulating miRNA to justify deferring surgery in Bethesda III/IV nodules, an NPV of at least 95% would generally be considered the minimum acceptable threshold. The current NPV values - 85.0% for miR-146b and 81.7% for miR-21 - fall short of that bar, reinforcing the discovery-stage characterization of these findings.

One of the major advantages of circulating miRNAs is their stability in serum and plasma as compared to mRNA-based biomarkers. Encapsulation into the secreted extracellular vesicles (exosomes, microvesicles) protects miRNAs against RNase degradation [33,34] or their association with Argonaute-2 protein complexes [35,36]. This stability enables standardization of pre-analytical procedures and confident dilution-based quantification by RT-qPCR. Details regarding the selection criteria for every cohort subset are reported with a row-based matrix style representation, including normalization against bovine fibroblast spike-ins (an example of QC mechanisms), technical triplicates and hemolysis screening to reduce pre-analytical and analytical variability. The within-run and between-run CVs were very acceptable for clinical biomarker assays (1.8 - 3.9%, respectively).

The use of an appropriate endogenous reference is essential for a reliable miRNA quantification. We preferentially selected miR-16 because it was shown to be stably expressed in thyroid-related serum specimens [11]. Nonetheless, miR-16 stability is decreased by hemolysis and inflammatory states, although formal validation with geNorm or NormFinder algorithms was not performed in our cohort. This is a restriction, and in future studies, more than one reference miRNA or spike-in control for normalization should be used. The clinical relevance of circulating miRNA biomarkers would have to be investigated in relation with existing tools used for tissue diagnosis. FNAB cytology is the current gold standard, but indeterminate results (Bethesda III and IV) occur in 15 - 30% of cases. To improve this risk stratification in this population, molecular classifiers like Afirma Gene Expression Classifier and ThyroSeq have emerged, achieving NPVs of 94 - 96% (37,38).

Limitations

Several limitations deserve explicit acknowledgment. Only surgically managed patients were enrolled, limiting the disease spectrum and likely artificially increasing sensitivity and specificity relative to a consecutive-referral cohort. Non-surgical patients, generally those with cytologically benign nodules, were ineligible, precluding estimation of false-negative rates in that subset.

The 1:1 case-control ratio produces a theoretical prevalence of 50%; at realistic PTC prevalence of 10 - 15%, PPV for the combined marker falls to 42.5 - 54.0%. Bootstrap correction quantifies optimism of +1.7% - +2.3% in sensitivity and +1.2% - +2.1% in specificity, but does not eliminate it; the wide bootstrap CI for the combined-model threshold (0.349 - 0.756) reflects genuine instability at n = 120. This is a single-center study, limiting generalizability to other Iraqi institutions and non-Middle Eastern populations. Only PTC was studied; utility of the panel in follicular, medullary, or anaplastic carcinoma is unknown. Formal geNorm/NormFinder validation of miR-16 as endogenous reference was not performed. The unmatched design and absence of covariate adjustment permit residual confounding. Subgroup analyses are exploratory and not intended as tests of effect modification.

Clinical implications

These are proof-of-concept results and should not justify immediate clinical adoption. The envisioned role of this panel, once validated, is as a complement to FNAB cytology for indeterminate nodules - not a substitute. Clinical translation will require external validation in a prospective consecutive cohort with Bethesda III/IV nodules, achievement of NPV ≥ 95% at plausible PTC prevalence (10 - 15%), direct comparison with Afirma and ThyroSeq, and a formal health-economic analysis. Future studies should include consecutive patients with indeterminate cytology, external validation cohorts, integration with TI-RADS ultrasonography risk assessment, and formal health-economic evaluations.

CONCLUSION

This study has shown that, in this Iraqi cohort, circulating miR-146b-5p and miR-21-5p are upregulated in PTC versus benign thyroid nodules (PTC 29) with individual AUCs of 0.874 and 0.831, respectively, and a combined AUC of 0.912 (bootstrap-corrected: 0.897). By combining the markers, the discrimination of tumors is improved over that seen with either marker alone, and their associations with tumor size, lymph-node metastasis and TNM stage indicate that the signals they detect contain information other than a simple positive malignancy flag. To be clear, these are early-stage findings. The design as a case-control, cutoff derived in-sample and single-center limits the generalizability. The logical next step is prospective validation in a cohort of consecutive screening patients with complete cytological stratification according to the Bethesda system - and at clinically realistic disease prevalence.

Acknowledgment:

The authors thank the staff of the Medical City Complex, Baghdad, for their assistance with patient recruitment and specimen processing.

Source of Funds:

This research received no specific grant from any funding agency in the public, commercial, or not-for-profit sectors. No pharmaceutical or other company was involved in study design, data collection, analysis, interpretation, or manuscript preparation.

Declaration of Generative AI in Scientific Writing:

No generative AI tools were used in the preparation of this manuscript.

Data availability:

De-identified raw Cq values, normalized fold-change data, and clinical variables used in all statistical analyses are available from the corresponding author upon reasonable request, subject to institutional data-sharing policies and ethical approval from the Middle Technical University IRB (MEC 214). No data have been deposited in a public repository owing to patient confidentiality requirements under Iraqi national data-protection regulations; data sharing is subject to a data-use agreement.

Code Availability:

The R scripts (version 4.2.1; RRID:SCR_001905) used for bootstrap optimism correction (1,000 iterations), calibration analysis (Hosmer-Lemeshow test, calibration slope, Brier score), and decision-curve analysis are available from the corresponding author upon reasonable request. SPSS syntax files (version 26.0; RRID: SCR_002865) for Mann-Whitney U tests, chi-squared tests, and Spearman's correlations are similarly available upon request.

Declaration of Interest:

The authors declare no conflicts of interest. Both authors had full access to all study data and take responsibility for the integrity of the data and the accuracy of the analysis.

References:

1. Haugen BR, Alexander EK, Bible KC, et al. 2015 American Thyroid Association Management Guidelines for Adult Patients with Thyroid Nodules and Differentiated Thyroid Cancer: The American Thyroid Association Guidelines Task Force on Thyroid Nodules and Differentiated Thyroid Cancer. Thyroid 2016 Jan 1; 26(1):1-133. (PMID: 26462967)

2. Cibas ES, Ali SZ. The 2017 Bethesda System for Reporting Thyroid Cytopathology. Thyroid 2017 Nov 1;27(11):1341-6. (PMID: 29091573)

3. Bongiovanni M, Spitale A, Faquin WC, Mazzucchelli L, Baloch ZW. The Bethesda System for Reporting Thyroid Cytopathology: a meta-analysis. Acta Cytol 2012;56(4):333-9. (PMID: 22846422)

4. Alexander EK, Kennedy GC, Baloch ZW, et al. Preoperative diagnosis of benign thyroid nodules with indeterminate cytology. N Engl J Med 2012 Aug 23;367(8):705-15. (PMID: 22731672)

5. Nicholson KJ, Roberts MS, McCoy KL, Carty SE, Yip L. Molecular Testing Versus Diagnostic Lobectomy in Bethesda III/IV Thyroid Nodules: A Cost-Effectiveness Analysis. Thyroid 2019 Sep 1;29(9):1237-43. (PMID: 31407625)

6. Nikiforov YE, Carty SE, Chiosea SI, et al. Highly accurate diagnosis of cancer in thyroid nodules with follicular neoplasm/suspicious for a follicular neoplasm cytology by ThyroSeq v2 next-generation sequencing assay. Cancer 2014 Dec 1;120(23):3627-34. (PMID: 25209362)

7. Paschke R, Cantara S, Crescenzi A, Jarzab B, Musholt TJ, Sobrinho Simoes M. European Thyroid Association Guidelines regarding Thyroid Nodule Molecular Fine-Needle Aspiration Cytology Diagnostics. Eur Thyroid J 2017;6(3):115-29. (PMID: 28785538)

8. Al-Timimi NMN, Baraaj AH. KI-67 as a predictive indicator of papillary thyroid cancer in Iraqi patients. Probl Endokrinol (Mosk) 2024;70(6):62-6. (PMID: 39868448)

9. Bartel DP. MicroRNAs: Genomics, Biogenesis, Mechanism, and Function. Cell 2004 Jan 23;116(2):281-97. (PMID: 14744438)

10. Calin GA, Croce CM. MicroRNA signatures in human cancers. Nat Rev Cancer 2006 Nov 12;6(11):857-66. (PMID: 17060945)

11. Mitchell PS, Parkin RK, Kroh EM, et al. Circulating microRNAs as stable blood-based markers for cancer detection. Proc Natl Acad Sci U S A 2008 Jul 29;105(30):10513-8. (PMID: 18663219)

12. Chou CK, Chen RF, Chou FF, et al. miR-146b is highly expressed in adult papillary thyroid carcinomas with high risk features including extrathyroidal invasion and the BRAF(V600E) mutation. Thyroid 2010 May 1;20(5):489-94. (PMID: 20406109)

13. Deng X, Wu B, Xiao K, et al. MiR-146b-5p promotes metastasis and induces epithelial-mesenchymal transition in thyroid cancer by targeting ZNRF3. Cell Physiol Biochem 2015 Jan 21;35(1): 71-82. (PMID: 25547151)

14. Meng F, Henson R, Wehbe-Janek H, Ghoshal K, Jacob ST, Patel T. MicroRNA-21 Regulates Expression of the PTEN Tumor Suppressor Gene in Human Hepatocellular Cancer. Gastroenterology 2007;133(2):647-58. (PMID: 17681183)

15. Yu S, Liu Y, Wang J, et al. Circulating microRNA profiles as potential biomarkers for diagnosis of papillary thyroid carcinoma. J Clin Endocrinol Metab 2012 Jun;97(6):2084-92. (PMID: 22472564)

16. Lee JC, Zhao JT, Clifton-Bligh RJ, et al. MicroRNA-222 and microRNA-146b are tissue and circulating biomarkers of recurrent papillary thyroid cancer. Cancer 2013 Dec 15;119(24):4358-65. (PMID: 24301304)

17. Mazeh H, Deutch T, Karas A, et al. Next-Generation Sequencing Identifies a Highly Accurate miRNA Panel That Distinguishes Well-Differentiated Thyroid Cancer from Benign Thyroid Nodules. Cancer Epidemiol Biomarkers Prev 2018 Aug 1;27(8):858-63. (PMID: 30049841)

18. Bossuyt PM, Reitsma JB, Bruns DE, et al. STARD 2015: An Updated List of Essential Items for Reporting Diagnostic Accuracy Studies. Clin Chem 2015 Dec 1;61(12):1446-52. (PMID: 26510957)

19. von Elm E, Altman DG, Egger M, et al; STROBE Initiative. The Strengthening the Reporting of Observational Studies in Epidemiology (STROBE) statement: guidelines for reporting observational studies. J Clin Epidemiol 2008 Apr;61(4):344-9. (PMID: 18313558)

20. Collins GS, Reitsma JB, Altman DG, Moons KGM. Transparent reporting of a multivariable prediction model for individual prognosis or diagnosis (TRIPOD): the TRIPOD statement. BMJ 2015 Jan 7;350. (PMID: 25569120)

21. Bustin SA, Benes V, Garson JA, et al. The MIQE guidelines: minimum information for publication of quantitative real-time PCR experiments. Clin Chem 2009 Apr 1;55(4):611-22. (PMID: 19246619)

22. Basolo F, Macerola E, Poma AM, Torregrossa L. The 5th edition of WHO classification of tumors of endocrine organs: changes in the diagnosis of follicular-derived thyroid carcinoma. Endocrine 2023 Jun 1;80(3):470-6. (PMID: 36964880)

23. Amin MB, Greene FL, Edge SB, et al. The Eighth Edition AJCC Cancer Staging Manual: Continuing to build a bridge from a population-based to a more "personalized" approach to cancer staging. CA Cancer J Clin 2017 Mar;67(2):93-9. (PMID: 28094848)

24. Kirschner MB, Kao SC, Edelman JJ, et al. Haemolysis during sample preparation alters microRNA content of plasma. PLoS One 2011 Sep 1;6(9):e24145. (PMID: 21909417)

25. Cheng HH, Yi HS, Kim Y, et al. Plasma processing conditions substantially influence circulating microRNA biomarker levels. PLoS One 2013 Jun 7;8(6):e64795. (PMID: 23762257)

26. Peltier HJ, Latham GJ. Normalization of microRNA expression levels in quantitative RT-PCR assays: identification of suitable reference RNA targets in normal and cancerous human solid tissues. RNA 2008 May;14(5):844-52. (PMID: 18375788)

27. Livak KJ, Schmittgen TD. Analysis of relative gene expression data using real-time quantitative PCR and the 2-ΔΔCT method. Methods 2001;25(4):402-8. (PMID: 11846609)

28. DeLong ER, DeLong DM, Clarke-Pearson DL. Comparing the Areas under Two or More Correlated Receiver Operating Characteristic Curves: A Nonparametric Approach. Biometrics 1988 Sep;44(3):837-45. (PMID: 3203132)

29. Kazlauskiene M, Klimaite R, Kondrotiene A, et al. Plasma miRNA-146b-3p, -222-3p, -221-5p, -21a-3p Expression Levels and TSHR Methylation: Diagnostic Potential and Association with Clinical and Pathological Features in Papillary Thyroid Cancer. Int J Mol Sci 2024 Aug 1;25(15):8412. (PMID: 39125979)

30. Samir Assaad R, Saad Ragab W, El Tayfi R, El Sheredy AG. Circulating microRNA-222 and microRNA-146b: a potential differentiating tool between benign and malignant thyroid nodules. Scand J Clin Lab Invest 2025;85(7):581-9. (PMID: 41195835)

31. Taganov KD, Boldin MP, Chang KJ, Baltimore D. NF-kappaB-dependent induction of microRNA miR-146, an inhibitor targeted to signaling proteins of innate immune responses. Proc Natl Acad Sci U S A 2006 Aug 15;103(33):12481-6. (PMID: 16885212)

32. Liu C, Yu J, Yu S, et al. MicroRNA-21 acts as an oncomir through multiple targets in human hepatocellular carcinoma. J Hepatol 2010 Jul;53(1):98-107. (PMID: 20447717)

33. Liang M, Yu S, Tang S, et al. A Panel of Plasma Exosomal miRNAs as Potential Biomarkers for Differential Diagnosis of Thyroid Nodules. Front Genet 2020 May 19;11:449. (PMID: 32508877)

34. Delcorte O, Craps J, Mahibullah S, et al. Two miRNAs enriched in plasma extracellular vesicles are potential biomarkers for thyroid cancer. Endocr Relat Cancer 2022 Jul 1;29(7):389-401. (PMID: 35521768)

35. Turchinovich A, Weiz L, Langheinz A, Burwinkel B. Characterization of extracellular circulating microRNA. Nucleic Acids Res 2011 Sep;39(16):7223-33. (PMID: 21609964)

36. Arroyo JD, Chevillet JR, Kroh EM, et al. Argonaute2 complexes carry a population of circulating microRNAs independent of vesicles in human plasma. Proc Natl Acad Sci U S A 2011 Mar 22; 108(12):5003-8. (PMID: 21383194)

37. Patel KN, Angell TE, Babiarz J, et al. Performance of a Genomic Sequencing Classifier for the Preoperative Diagnosis of Cytologically Indeterminate Thyroid Nodules. JAMA Surg 2018;153(9): 817-24. (PMID: 29799911)

38. Nikiforova MN, Mercurio S, Wald AI, et al. Analytical performance of the ThyroSeq v3 genomic classifier for cancer diagnosis in thyroid nodules. Cancer 2018;124(8):1682-1690. (PMID: 29360127)

Additional material can be found online at:
http://supplementary.clin-lab-publications.com/260451/